and thoracic ganglia[16–19]. GIH has been the primary regulator of ovarian growth in *Oziotelphusa*[20]. Eyestalk-ablated crustaceans show accelerated ovarian growth[11,20] and increased MF levels in hemolymph[21,22]. The stimulatory action of MF on ovarian maturation could have been due to stimulation of GSH synthesis and release or inhibition of release of the GSH antagonist (GIH) or direct action of MF on ovary. It is not yet known how hemolymph levels of GIH and GSH change during the reproductive cycle of crustaceans, since a sensitive assay for GIH and GSH does not exist. It could be that all the three hormones (GIH, GSH and MF) are very important in regulating the timing of onset of reproduction in crustaceans. Studies are underway in this laboratory to test the effectiveness of MF in inducing ovarian development and spawning in broodstock females of aquaculturally important crustacean species.

1. Le Roux, A., *C. R. Hebd. Acad. Sci. Ser. D. Sci. Nat.*, 1968, **266**, 1414–1417.
2. Taketomi, Y., Motono, M. and Miyawaki, M., *Cell Biol. Int. Rep.*, 1989, **13**, 463–469.
3. Laufer, H., Landau, M. and Homola, E., *Adv. Invertebr. Reprod.*, 1986, **4**, 135–143.
4. Laufer, H., Borst, D., Baker, F. C., Carrasco, C., Sinkus, M., Reuter, C. C., Tsai, L. W. and Schooley, D. A., *Science*, 1987, **235**, 202–205.
5. Laufer, H., Landau, M., Homola, E. and Borst, D. W., *Insect Biochem.*, 1987, **17**, 1129–1131.
6. Tobe, S. S., Young, D. A. and Khoo, H. W., *Gen. Comp. Endocrinol.*, 1989, **73**, 342–353.
7. Yudin, A. I., Diener, R. A., Clark, W. H. and Chang, E. S., *Biol. Bull.*, 1980, **159**, 760–772.
8. Tamone, S. L. and Chang, E. S., *Gen. Comp. Endocrinol.*, 1993, **89**, 425–432.
9. Hinsch, G. W., *Trans. Am. Microsc. Soc.*, 1980, **99**, 317–322.
10. Borst, D. W., Laufer, H., Landau, M., Chang, E. S., Hertz, W. A., Baker, F. C. and Schooley, D. A., *Insect Biochem.*, 1987, **17**, 1123–1127.
11. Reddy, P. S., *Trop. Freshwater Biol.*, 1990, **2**, 213–222.
12. Van Harreveld, A., *Proc. Soc. Exp. Biol. Med.*, 1936, **34**, 428–432.
13. Reddy, V. V., Doctoral dissertation, S. V. University, Tirupati, India, 1980, pp. 1–140.
14. Bancroft, J. D. and Stevens, A., *Theory and Practice of Histological Techniques*, Churchill Livingstone, New York, 1982, 2nd edn.
15. Tsukimura, B. and Kamemoto, F. I., *Aquaculture*, 1991, **92**, 59–66.
16. Panouse, J. B., *C. R. Hebd. Seanc. Acad. Sci. Paris*, 1943, **217**, 553–555.
17. Panouse, J. B., *C. R. Hebd. Seanc. Acad. Sci. Paris*, 1944, **218**, 293–294.
18. Otsu, T., *Embryologia*, 1963, **8**, 1–20.
19. Gomez, R., *Naturwissenschaften*, 1965, **52**, 216–217.
20. Reddy, P. S., Bhagyalakshmi, A. and Ramamurthi, R., *Toxicol. Lett.*, 1983, **18**, 273–276.
21. Landau, M., Laufer, H. and Homola, E., *Invertebr. Reprod. Dev.*, 1989, **16**, 165–168.
22. Tsukimura, B. and Borst, D. W., *Gen. Comp. Endocrinol.*, 1992, **86**, 297–303.

ACKNOWLEDGEMENTS. P.S.R. thanks the Management, Pondicherry University, Pondicherry for granting sabbatical leave during which the present work was carried out and the Staff of Zoology Department, Sri Venkateswara University, Tirupati for critical support. We are grateful to Prof. Ernest S. Chang, Bodega Marine Laboratory, University of California at Davis (USA) for his encouragement and advice and to Prof. Hans Laufer, University of Connecticut for his critical comments. Portions of this work are a result of research sponsored by the Rockefeller Foundation Biotechnology Carrier Fellowship to P.S.R.

Received 12 September 1997; revised accepted 28 October 1997

Ion microprobe $^{207}Pb/^{206}Pb$ zircon ages for gneiss-granitoid rocks from Bundelkhand massif: Evidence for Archaean components

M. E. A. Mondal, K. K. Sharma*, A. Rahman* and J. N. Goswami

Physical Research Laboratory, Ahmedabad 380 009, India
*Wadia Institute of Himalayan Geology, Dehra Dun 248 001, India

Radiometric $^{207}Pb/^{206}Pb$ ages of individual zircons from the Bundelkhand massif, central India, have been determined by an ion microprobe. Samples from various major litho-units, viz. the granite gneiss, hornblende-, biotite- and leuco-granitoid are included in this study. The results provide evidence for the presence of Archaean crustal components within this massif. Zircons with ages of 3.0 to 3.2 Ga occur as xenocrysts in a sample of granite gneiss from Lalitpur having a minimum formation age of 2.5 Ga. Another sample of a highly deformed gneiss from Babina has a well-defined age of 2.7 Ga. Emplacement of hornblende-granitoid and biotite-granitoid took place in quick succession at ~ 2.5 Ga. No firm age for the youngest plutonic component, the leuco-granitoid, could be obtained due to poor recovery of zircons suitable for analysis. The geochronological data confirm the suggestion, based on geochemical studies, that the gneisses and the granitoids in this region represent Archaean and post-Archaean components, respectively.

THE Bundelkhand 'massif' is a composite granite-gneiss province occupying an area of about 26,000 km^2 in the central portion of the Indian shield covering the southern parts of Uttar Pradesh and the north-eastern parts of Madhya Pradesh (Figure 1). The massif is unconformably overlain by the meta-sedimentary and associated meta-volcanic rocks of the Bijawar Group in the south and south-east, and by the still younger Vindhyan Supergroup of sedimentary rocks in the south-east, south and west. The Indo-Gangetic alluvium covers much of the northern portion of the massif. The geology of the region has

been reviewed by Basu[1]. The bulk of the Bundelkhand massif comprises of various phases of undeformed granitoids which have intruded into a basement comprising of gneisses, banded iron formations (BIF), metasediments, and mafic and ultramafic rocks. At places the basement components also occur as small enclaves. The massif is traversed by two prominent sets of lineaments having in general NE and NW trends filled with quartz veins and mafic dykes, respectively (Figure 1).

The massif has a complex geological history of evolution as demonstrated by the contrasting litho-units and polyphase deformational events[2], typical of many Archaean–Palaeoproterozoic cratons. However, detailed geochemical and petrological studies have not been attempted yet to unravel the genesis of the different litho-units and their evolution in the regional tectonic framework. Based on a study of the granitoids from different parts of the massif in and around Mahoba and Lalitpur, Rahman and Zainuddin[3] and Mondal and Zainuddin[4] provided geochemical data of different granitoid suites to constrain the processes for the formation of the granitoids. Mondal and Zainuddin[5] proposed that the granitoids were emplaced in a volcanic arc tectonic setting associated with subduction of an oceanic plate and noted that their trace element abundance patterns resemble post-Archaean granitoids. Sarkar *et al.*[6] have suggested that the granitoids have post-tectonic geochemical characteristics. The earlier crust into which the granitoids were emplaced have remained unexplored. Sharma and Rahman[7] have reported highly fractionated rare earth element patterns with heavy rare earth depletion in the gneissic samples and proposed that the gneisses may belong to Archaean tonalite–trondhjemite–granodiorite (TTG) suites and represent the early crust in the Bundelkhand. A similar suggestion has also been made by Sarkar *et al.*[8]. The only geochronological data for samples from the Bundelkhand massif available so far are several Rb–Sr whole rock and mineral ages for different granitoids and one gneissic phase[8,9].

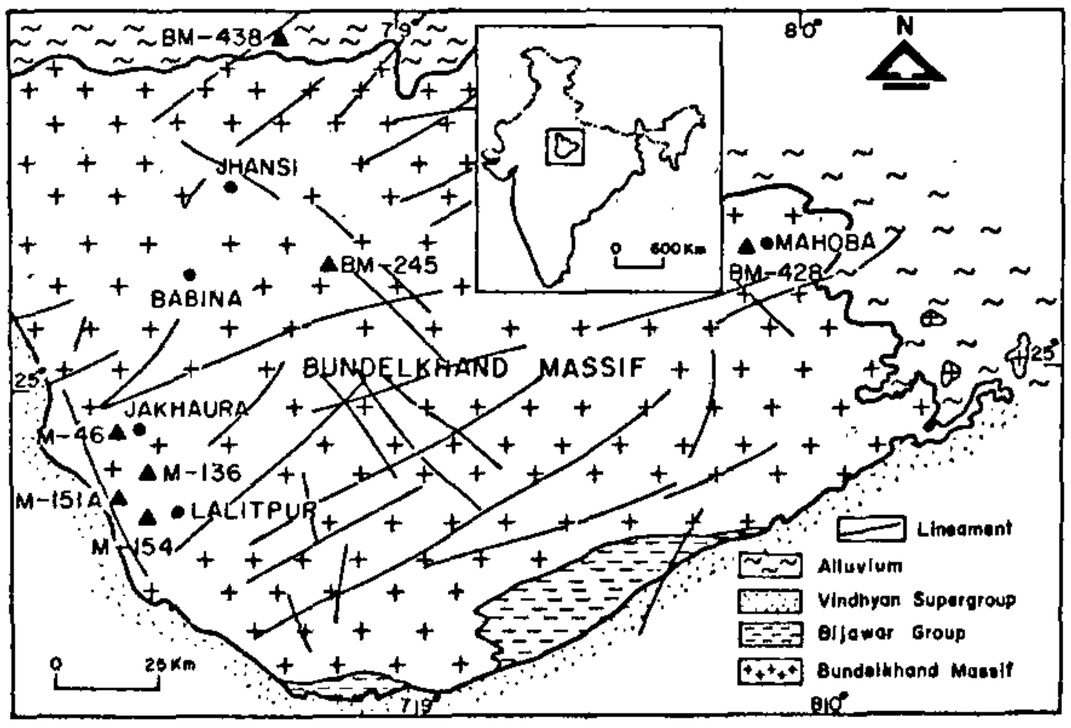

Figure 1. Geological map of the Bundelkhand massif in central India (after Basu[1]). The approximate geographical location of the massif is shown in the inset. The filled triangles indicate sample location. Some of the prominent field locations are also indicated (filled circle).

In this paper, we present initial results obtained from $^{207}Pb/^{206}Pb$ dating of single zircons by an ion microprobe. We have included representative samples from all the major lithologies of Bundelkhand massif. Representative gneissic samples from three well-separated locales were analysed. In addition, four granitoid phases representing hornblende-granitoid, biotite-granitoid and leuco-granitoid were selected to obtain a younger age limit of the massif. The samples were collected from areas close to Babina, Karera, Mahoba and Lalitpur (Figure 1). The gneisses from Babina and Karera (BM-245 and BM-438, respectively) exhibit isoclinal folding of the biotite-rich and quartzo-feldspathic bands. The gneisses are grey-coloured and are generally uniform in mineral composition with quartz and plagioclase as the dominant mineral phases; K-feldspar at places occurs as phenocryst. Biotite is ferromagnesian in nature and often alters to chlorite[7]. Accessory minerals include apatite and zircon. The different granitoids have similar mineralogy except for the leuco-granitoid which does not have hornblende. The common primary mineral phases of the granitoids are quartz, plagioclase feldspar, microcline and biotite; apatite, zircon, sphene and magnetite are the common accessories. The granitoids range in composition from quartz diorite to syenogranite and evolve with time from dominantly metaluminous to peraluminous geochemistry and correspond to calc-alkaline trend[5], whereas trondhjemite trend can be discerned for the gneisses[7,8].

Utmost care was taken to collect fresh rock samples; in most cases samples were collected from the quarries. The samples were processed using standard techniques[10,11] to obtain zircon grains. They were crushed to ≤ 250 micron size and the crush was passed through aqueous sodium-polytungstate solution of density 3 g/cm^3; the heavier fraction was isodynamically separated to obtain strongly non-magnetic fraction from where zircons were hand-picked using a binocular microscope. The zircons were mounted in epoxy and polished to expose the interior of the crystals. Optically clear, fractureless, inclusion-free domains of zircon were selected for analysis. In the gneisses, the zircons occur mainly as euhedral to subhedral crystals with frequent zonation; a few exhibit subrounded core structures. The zircon population of the granitoids is morphologically homogeneous and shows short prismatic crystal habit with zoning. The sample of hornblende granitoid yielded many good zircons that are mostly transparent, colourless to pale brown and euhedral. The gneiss sample collected from Karera (BM-438) did not yield good zircons, while only a couple of good zircons, suitable for analysis, could be found in the case of leuco-granitoid (M-136). Photo-

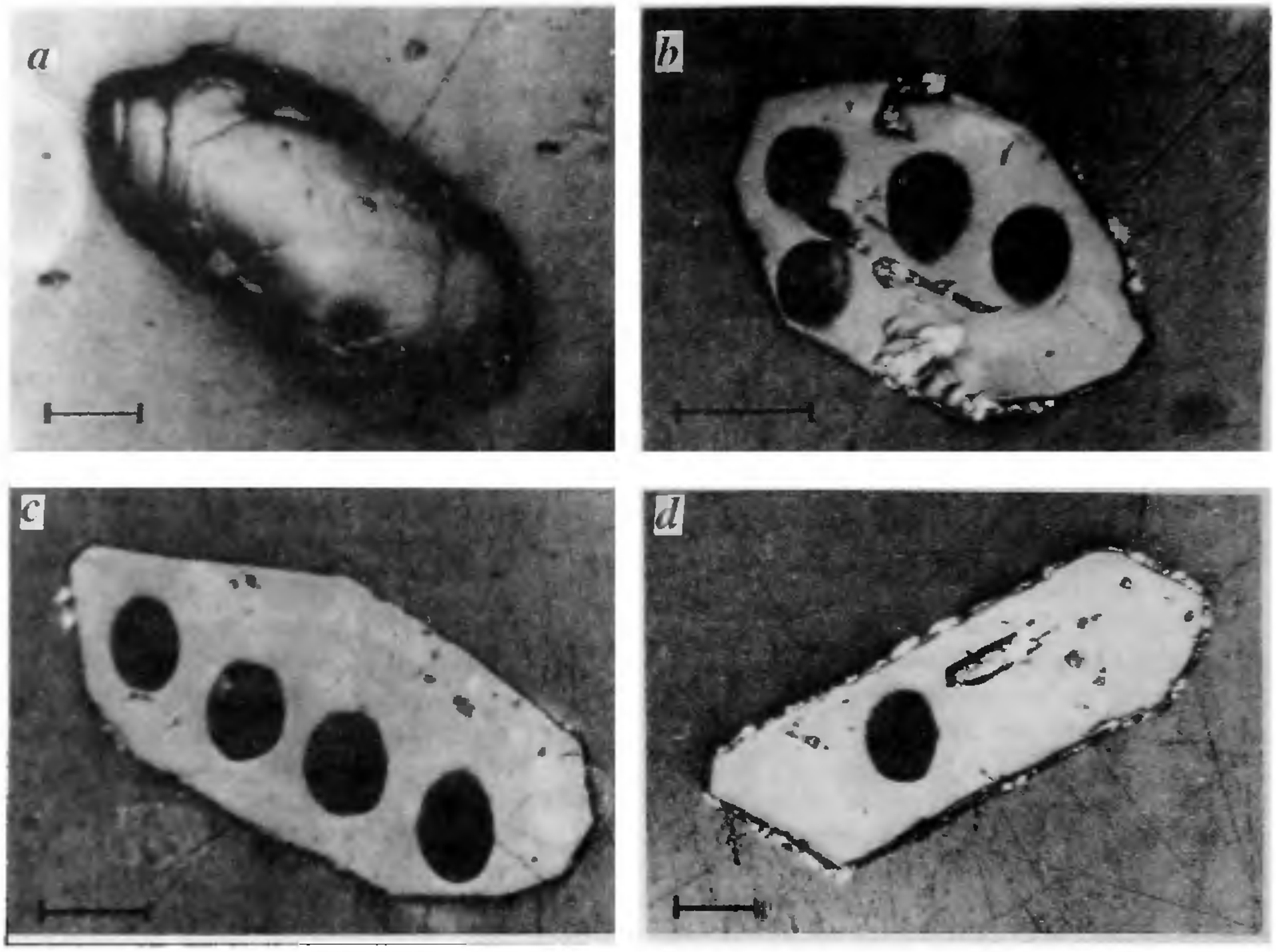

Figure 2. Reflected light photomicrographs of zircons recovered from the gneissic sample M-151A. Sputter holes caused by primary ion beam during Pb-isotopic analysis can be seen in several grains (*b*, *c* and *d*). The scale bar in each case is 50 μm.

micrographs of several analysed zircons are shown in Figure 2.

Radiogenic $^{207}Pb/^{206}Pb$ isotopic composition of carefully selected domain of individual zircons has been determined using a Cameca ims 4f ion microprobe following procedures described earlier[10,11]. Briefly, a 7 nA focused primary beam of $^{16}O^-$ was used to sputter ~ 20 micron domain of individual zircons. The secondary ions were mass analysed at a high mass resolving power ($M/\Delta M = 4500$), sufficient to resolve all the significant isobaric molecular interferences in the Pb-isotope mass spectrum. Each analysis consists of 15 blocks of data and each block of data consists of 5 scans through the mass sequence $^{204}(Zr_2O)$, ^{204}Pb, ^{206}Pb, ^{207}Pb, $^{208}(HfO_2)$ and ^{208}Pb, after which an automatic recalibration of magnetic field was performed. The age for each analysis is based on the weighted mean radiogenic $^{207}Pb/^{206}Pb$ ratio obtained from the data of the 15 quasi-independent blocks. As we do not include U isotope in our analysis routine, we do not have detailed information on the Pb-loss history of the analysed sample. Several objective criteria are therefore applied to identify Pb-loss as well as multiple age components within our data set (see refs 10 and 11 for details). As a precaution we exclude analysis characterized by high common Pb component (high $^{204}Pb/^{206}Pb$ ratio) from our data set, thus eliminating those analyses that show obvious evidence for Pb exchange. The age of a sample is derived by pooling the data (at block level) for all the analyses identified as belonging to the 'magmatic' component and obtaining a grand mean $^{207}Pb/^{206}Pb$ ratio, which then defines the 'minimum' age of the sample. However, if the analyses show a sharp cut-off at higher radiogenic $^{207}Pb/^{206}Pb$ ratios, the 'minimum' age closely approximates the 'true age' of the sample[10,11].

$^{207}Pb/^{206}Pb$ ages for different lithologies of the Bundelkhand massif, obtained in this study, are given in Table 1. We have carried out six analyses on five zircons from the highly deformed gneissic sample BM-245; five of these analyses have low common Pb component and they are included in Table 1. Four of these analyses belong to a single age group and the 57 blocks of data obtained from these analyses yielded a weighted mean radiogenic $^{207}Pb/^{206}Pb$ ratio of 0.18548 ± 26, equivalent to an age of 2703 ± 3 Ma (error quoted here and the rest of the text is 1σ). The somewhat lower age for the fifth analyses (#2A) is probably due to partial Pb-loss. We, however, note that the inclusion of this

Table 1. Ion microprobe Pb-isotopic data for zircons from Bundelkhand massif

Analysis no.+	Measured $^{204}Pb/^{206}Pb$	Measured $^{207}Pb/^{206}Pb$	Total ^{206}Pb counts	^{206}Pb (ppm)*	U (ppm)$	$^{207}Pb/^{206}Pb$*	Age (Ma)**
Sample: BM-245 (Gneiss, Babina)							
2A	0.00022	0.1798	157735	313	725	0.1770 ± 17‡	2625 ± 16
2B	0.00025	0.1882	123195	273	611	0.1852 ± 13‡	2700 ± 12
3	0.00038	0.1842	135565	221	506	0.1796 ± 12‡	2649 ± 11
5	n.d.	0.1858	327229	1122	2504	0.1858 ± 03‡	2705 ± 2
6	0.00038	0.1880	79605	232	524	0.1834 ± 22‡	2684 ± 20
Sample: M-151A (Gneiss, Panchwara village, Lalitpur)							
1	0.00056	0.1776	184050	328	782	0.1705 ± 18	2563 ± 18
4	0.00024	0.2389	71240	154	291	0.2362 ± 22§	3094 ± 15
5	0.00046	0.1677	61645	133	330	0.1620 ± 24	2476 ± 25
6	0.00019	0.2415	177660	455	852	0.2394 ± 12§	3116 ± 8
7A	0.00022	0.2520	96000	252	459	0.2496 ± 28§	3182 ± 18
7C	0.00007	0.2514	214890	386	703	0.2507 ± 16§	3189 ± 10
7D	0.00008	0.2518	313505	334	607	0.2509 ± 08§	3190 ± 4
8	0.00027	0.1739	121705	226	539	0.1705 ± 16	2563 ± 15
10	0.00032	0.1711	140535	335	811	0.1671 ± 16	2529 ± 16
12B	0.00004	0.1697	316725	345	827	0.1692 ± 08	2550 ± 7
14	0.00049	0.1656	94460	211	531	0.1594 ± 20	2450 ± 20
15	0.00063	0.1746	121800	215	521	0.1667 ± 22	2525 ± 22
16	0.00032	0.1633	46915	135	340	0.1594 ± 31	2449 ± 32
18	0.00042	0.1658	100615	272	681	0.1605 ± 16	2461 ± 16
21	0.00043	0.1685	146345	383	945	0.1632 ± 12	2489 ± 12
22	0.00038	0.1675	87880	223	553	0.1627 ± 19	2484 ± 19
28A	0.00022	0.2254	180580	473	929	0.2228 ± 15§	3002 ± 10
30	0.00016	0.1701	151225	229	528	0.1682 ± 13	2540 ± 13
Sample: BM-428 (Hornblende-granitoid, Mahoba)							
1	0.00011	0.1708	63090	234	561	0.1694 ± 22	2551 ± 22
2A	0.00033	0.1665	70110	496	1231	0.1623 ± 21	2480 ± 22
2B	0.00059	0.1714	44260	483	1188	0.1639 ± 32	2496 ± 33
2C	0.00045	0.1579	104920	465	1218	0.1522 ± 37	2371 ± 41
3	0.00051	0.1551	53255	375	1002	0.1485 ± 30	2329 ± 34
5	0.00050	0.1685	50685	482	1195	0.1623 ± 31	2479 ± 33
7	0.00032	0.1639	153935	588	1477	0.1599 ± 14	2454 ± 15
10B	0.00046	0.1559	15335	264	698	0.1501 ± 89	2347 ± 101
Sample: M-46 (Hornblende-granitoid, Jakhaura)							
1A	0.00062	0.1698	70410	260	645	0.1620 ± 23	2477 ± 24
1B	0.00034	0.1697	75685	179	436	0.1655 ± 22	2512 ± 22
2A	0.00055	0.1684	31065	86	214	0.1615 ± 46	2471 ± 48
5	0.00023	0.1664	64280	120	296	0.1635 ± 24	2493 ± 25
6	0.00050	0.1739	70185	147	356	0.1676 ± 21	2534 ± 21
7	0.00016	0.1684	84210	179	436	0.1664 ± 20	2522 ± 20
8	0.00046	0.1693	88015	184	454	0.1635 ± 19	2492 ± 20
9	0.00051	0.1701	45380	102	252	0.1637 ± 34	2494 ± 35
10A	0.00012	0.1685	122935	263	637	0.1670 ± 14	2528 ± 14
10B	0.00010	0.1602	120455	338	853	0.1589 ± 58	2444 ± 62
11A	0.00030	0.1709	54070	124	301	0.1671 ± 28	2529 ± 28
11B	0.00010	0.1701	71050	125	300	0.1688 ± 19	2546 ± 18
11C	0.00029	0.1694	75375	147	358	0.1657 ± 23	2515 ± 23
Sample: M-154 (Biotite-granitoid)							
16B	0.00044	0.1676	113265	199	495	0.1621 ± 18	2477 ± 18
17A	0.00041	0.1718	167640	240	582	0.1667 ± 13	2524 ± 13
17B	0.00020	0.1688	146030	279	678	0.1664 ± 17	2521 ± 17
17C	0.00028	0.1678	118585	359	881	0.1642 ± 14	2500 ± 14
20	0.00033	0.1653	125925	289	721	0.1612 ± 13	2468 ± 13

+Alphabets refer to multiple analyses of single zircons.
$Calculated value based on the assumption that the sample has remained a closed system.
*Radiogenic value corrected using model common Pb for an age of 3.2 Ga (data identified by the symbol §), 2.7 Ga (data identified by the symbol ‡) and 2.55 Ga for rest of data following Cumming and Richards (ref. 12).
**Errors are 1σ.
n.d., No ^{204}Pb was detected.

analysis will not significantly alter the deduced age of the sample.

We have conducted 18 analyses on sixteen zircons from another gneissic sample M-151A. The results clearly show a two-component system; six analyses conducted on four zircons yielded ages ranging from 3.0 to 3.2 Ga, while the other twelve zircons have ages clustering around 2.5 Ga (see Table 1 and Figure 3). The data for the zircons belonging to the younger age group yielded a weighted mean radiogenic $^{207}Pb/^{206}Pb$ ratio of 0.16639 ± 43, equivalent to an age of 2522 ± 5 Ma. We obtain a well-defined age of 3189 ± 5 Ma for one of the zircons belonging to the older age group; three analyses conducted on this grain (#7A, C and D; see Table 1) yielded concordant ages within the limits of our experimental uncertainty.

Eight analyses were conducted on six zircons from the sample of hornblende-granitoid BM-428. Five of these analyses (#1, 2A, 2B, 5 and 7; see Table 1) belong to a single age group and yielded a weighted mean radiogenic $^{207}Pb/^{206}Pb$ ratio of 0.16256 ± 68, equivalent to an age of 2482 ± 7 Ma. The much lower ages for the remaining three analyses are indicative of partial Pb-loss in these cases. All the thirteen analyses conducted on nine zircons from the second sample of hornblende-granitoid M-46, belong to a single age group, and yielded a mean age of 2516 ± 4 Ma. We have conducted five analyses on three zircons from the sample of biotite-granitoid M-154. Three analyses carried out on a single zircon (#17A, B and C; see Table 1) yielded a very well-defined age of 2521 ± 6 Ma. Even though the other two zircons have slightly lower ages, they are not inconsistent with the age deduced above. We could find only two zircons suitable for analysis from the sample of the leuco-granitoid (M-136); they have ages of 2429 ± 30 Ma and 2108 ± 36 Ma, respectively. The lower age of 2108 ± 36 Ma may reflect Pb-loss from this grain which appears to be metamict when viewed in transmitted light.

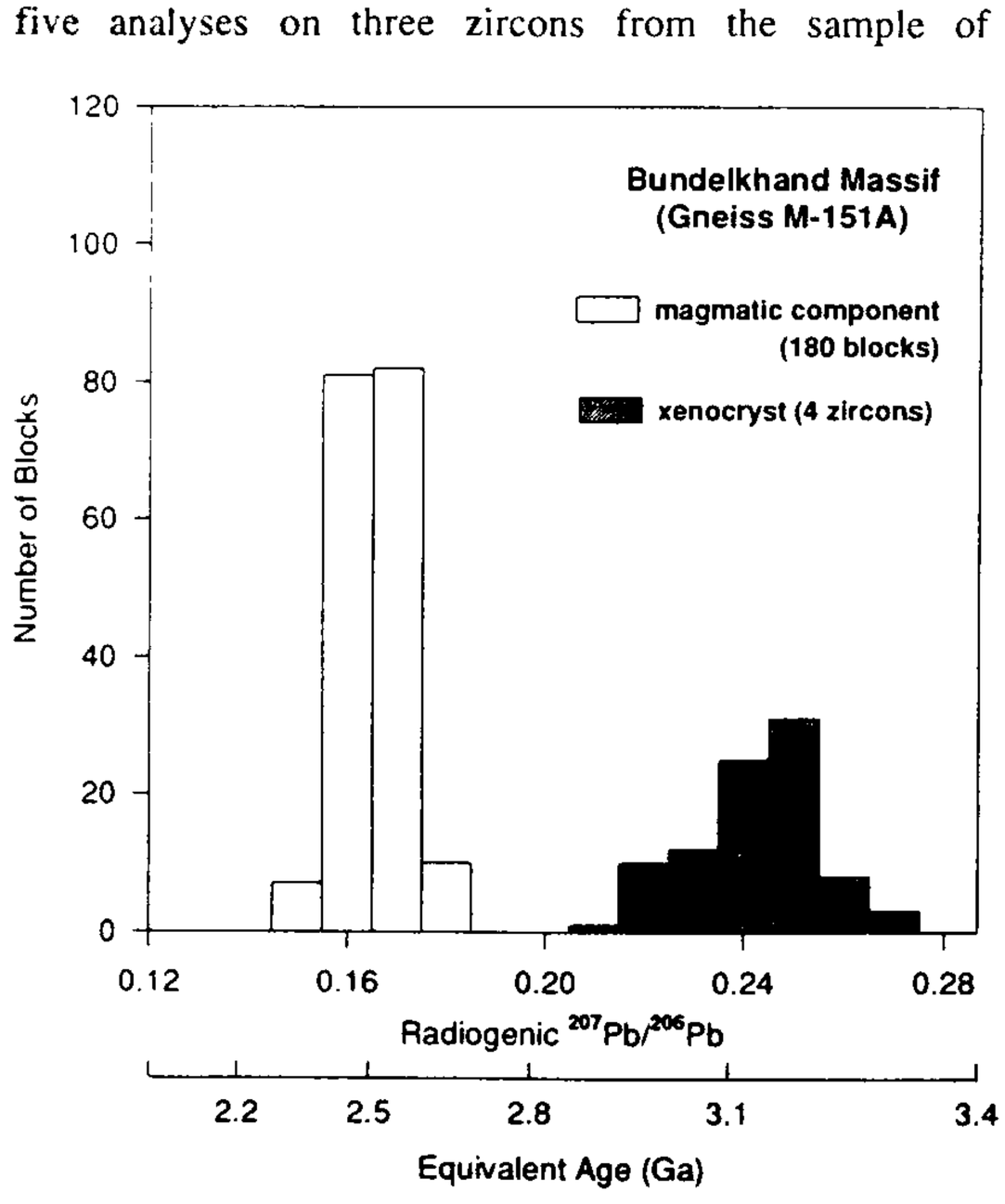

Figure 3. Histogram of radiogenic $^{207}Pb/^{206}Pb$ block data for the gneissic sample M-151A collected from Panchwara village near Lalitpur (see Figure 1).

The results obtained represent the first zircon geochronological data for the Bundelkhand massif and provide evidence for the presence of Archaean components in this region. We interpret the older ages of 3.0 to 3.2 Ga, obtained for a sub-set of zircons in the gneissic sample M-151A, as a xenocrystic component. The zircons belonging to this age group are characterized by euhedral to subhedral morphology (Figure 2 *a–c*) and exhibit probable sub-rounded core structure in a couple of cases (Figure 2 *a*). In contrast, the main zircon population from this sample belonging to the 2.5 Ga age group have distinctive euhedral, prismatic, crystal habit (Figure 2 *d*) and also exhibit frequent zonation, as can be seen in transmitted light, indicating a magmatic origin. The age of 2.7 Ga for the highly deformed gneiss BM-245 confirms the suggestion made by Sharma and Rahman[7], based on geochemical consideration, that the gneisses may belong to the Archaean TTG suite. The presence of zircons of two age groups (~ 3.1 Ga and 2.5 Ga) in the gneiss from Lalitpur (M-151A) may be attributed to either impregnation of older gneissic component by younger granitic component or xenocrystic nature of the older zircons in the rock that crystallized at 2.5 Ga. In either case, the presence of zircon with ages of 3.0–3.2 Ga in the Lalitpur gneiss and of 2.7 Ga in Babina gneiss provides evidence for an Archaean crustal component in the Bundelkhand massif. A Rb–Sr age of 3.5 Ga for a gneissic phase from the Babina area has been reported recently by Sarkar *et al.*[8]. Our inability to find zircon older than 2.7 Ga in another gneissic phase collected from this area points towards the need for reassessing the Rb–Sr data. The age data for the hornblende- and biotite-granitoids indicate them to be nearly contemporaneous and suggest that a large-scale granitoid magmatism in this region took place around 2.5 Ga. We plan to further investigate the possible presence of older crustal components in the Bundelkhand massif and their relation, if any, with the Archaean components in the Aravalli Craton[11] bordering the western side of this massif. Since the highly deformed gneiss is intruded by the undeformed ~ 2.5 Ga old hornblende-granitoid, the age of ~ 2.5 Ga provides a limiting value on the time of this deformation event. In the absence of comprehensive zircon age data for the leuco-granitoid, the

youngest plutonic unit in this region, we cannot conclusively establish the time for the end of granitoid magmatism and stabilization of the massif. However, if the 2429 ± 30 Ma age for the single zircon from this unit may be taken to be representative of the formation age of the leuco-granitoid, the time of stabilization of the massif is very close to the inferred stabilization age of 2.5 Ga for the Aravalli Craton[11] bordering the western side of the Bundelkhand massif.

1. Basu, A. K., *Rec. Geol. Surv. India*, 1986, **117**, 61–124.
2. Sharma, R. P., in *Geology of Vindhyachal* (eds Valdiya, K. S., Bhatia, S. B. and Gaur, V. K.), Hindustan Publ. Co., New Delhi, 1982, pp. 30–40.
3. Rahman, A. and Zainuddin, S. M., *J. Geol.*, 1993, **101**, 413–419.
4. Mondal, M. E. A. and Zainuddin, S. M., *J. Geol. Soc. India*, 1997, **50**, 69–74.
5. Mondal, M. E. A. and Zainuddin, S. M., *Terra Nova*, 1996, **8**, 532–539.
6. Sarkar, A., Bhalla, J. K., Bishui, P. K., Gupta, S. N., Singhai, R. K. and Upadhaya, T. P., *Indian Minerals*, 1994, **48**, 103–110.
7. Sharma, K. K. and Rahman, A., *Curr. Sci.*, 1995, **69**, 613–616.
8. Sarkar, A., Paul, D. K. and Potts, P. J., *Rec. Res. Geol.*, 1996, **16**, 76–92.
9. Sarkar, A., Trivedi, J. R., Gopalan, K., Singh, P. N., Singh, B. K., Das, A. K. and Paul, D. K., *Indian J. Earth Sci.*, CEISM Seminar Volume, 1984, pp. 64–72.
10. Wiedenbeck, M. and Goswami, J. N., *Geochim. Cosmochim. Acta*, 1994, **58**, 2135–2141.
11. Wiedenbeck, M., Goswami, J. N. and Roy, A. B., *Chem. Geol.*, 1996, **129**, 325–340.
12. Cumming, G. L. and Richards, J. R., *Earth Planet. Sci. Lett.*, 1975, **28**, 155–171.

ACKNOWLEDGEMENTS. We thank Mr M. P. Deomurari, Ms N. Sinha and Mr V. G. Shah of PRL for technical assistance during various phases of this study. K.K.S. thanks DST, New Delhi for financial assistance and the Director, WIHG for facilities.

Received 15 April 1997; revised accepted 20 October 1997

Seismotectonics of northeastern India

T. N. Gowd, S. V. Srirama Rao and K. B. Chary

National Geophysical Research Institute, Uppal Road, Hyderabad 500 007, India

Intraplate seismicity accounts for about 20% of the earthquake activity of northeastern India. The Shillong plateau, northern Bengal basin, Tripura fold belt and Kopili lineament zone together contribute 87% of the intraplate seismicity of the region while Upper Assam is free from earthquake activity. The high seismic activity of the Shillong plateau appears to be related to the gently northward dipping seismogenic thrust fault, rupturing of which caused the great Assam earthquake of 1897. Excessive stresses induced in the Shillong plateau, northern Bengal basin and the Kopili lineament zone due to underthrusting along the Shillong thrust fault and beneath the eastern Himalaya appear to be the root cause of the intraplate seismicity in the region. The entire intraplate area excepting Upper Assam and the Kopili lineament zone is identified as a separate stress region characterized by a mean S_{Hmax} orientation of N3°E. The mean S_{Hmax} orientation in Upper Assam is N26°E. The Kopili lineament zone forms a broad stress boundary between them. Fractures/faults associated with only the Sylhet lineament, *Eocene* limestone hinge, Kopili, Tista and Padma lineaments are favourably oriented for their reactivation in strike-slip mode. The fact that only the first three amongst them are seismically active may be attributed to the high stresses induced in the northen Bengal basin and Kopili lineament zone. It appears that the crust beneath Upper Assam is a rigid block with unfavourably oriented fractures/faults, and is being deformed at a much slower strain rate, and as a result it is seismically stable.

THE northeastern region of India is seismically one of the most active regions in the world[1]. Two among a dozen largest earthquakes (M 8.7) of the world occurred in this part of the country, one in 1897 in the Shillong plateau and another in 1950 in the Assam syntaxis. The region is situated at the northeastern corner of the Indian plate and comprises of plate boundary zones and intraplate area. It is bounded by the plate boundary zones of the eastern Himalaya in the north, Assam syntaxis in the northeast and northern Indoburman ranges of the Naga-Disang and Arakan-Yoma thrust fold belt in the east (Figure 1). The intraplate part of the region includes seven tectonic units namely, the Shillong plateau, Bengal basin, Tripura fold belt, Kopili lineament zone, Rajmahal-Garo gap, Brahmaputra valley and Upper Assam. Because of its critical location, the region has come under the grip of a set of complicated tectonic forces ever since the collision of India with Eurasia. It is fairly well understood that the seismicity of the plate boundary zones of the eastern Himalaya and Indoburman ranges is closely related to and controlled by the collision tectonic processes. However, intraplate seismicity of the region is not yet fully understood, and needs further study. The present paper is directed towards that goal.

A catalogue of earthquakes of northeastern India ($M \geq 4.5$) for the period 1897–1992 has been compiled by Gowd *et al.*[2] using the earthquake data base published by Gupta *et al.*[1] for the period 1897–1962 and NOAA publications for the period 1963 onwards. The catalogue indicates that 710 earthquakes of $M \geq 4.5$ including two earthquakes of M 8.7, 16 earthquakes having magnitude in the range of 7.0 to 7.9 and 53 earthquakes having magnitude in the range of 6.0 to 6.9 occurred in